The American Journal of Pathology, Vol. 177, No. 5, November 2010

DOI: 10.2353/ajpath.2010.100279

Cell Injury, Repair, Aging and Apoptosis

Evidence of Oxidative Stress in the Pathogenesis of Fuchs Endothelial Corneal Dystrophy

Ula V. Jurkunas,*†‡ Maya S. Bitar,*‡
Toshinari Funaki,*‡ and Behrooz Azizi*‡

From the Schepens Eye Research Institute, Boston; the Massachusetts Eye and Ear Infirmary,† and the Department of Ophthalmology, Harvard Medical School,‡ Boston, Massachusetts*

Fuchs endothelial corneal dystrophy (FECD) is a progressive, blinding disease characterized by corneal endothelial (CE) cell apoptosis. Corneal transplantation is the only measure currently available to restore vision in these patients. Despite the identification of some genetic factors, the pathophysiology of FECD remains unclear. In this study, we observed a decrease in the antioxidant response element-driven antioxidants in FECD corneal endothelium. We further demonstrated that nuclear factor erythroid 2-related factor 2, a transcription factor known to bind the antioxidant response element and activate antioxidant defense, is down-regulated in FECD endothelium. Importantly, we detected significantly higher levels of oxidative DNA damage and apoptosis in FECD endothelium compared with normal controls and pseudophakic bullous keratopathy (iatrogenic CE cell loss) specimens. A marker of oxidative DNA damage, 8-hydroxy-2′-deoxyguanosine, colocalized to mitochondria, indicating that the mitochondrial genome is the specific target of oxidative stress in FECD. Oxidative DNA damage was not detected in pseudophakic bullous keratopathy corneas, whereas it colocalized with terminal deoxynucleotidyl transferase-mediated dUTP nick-end labeling-positive cells in FECD samples. *Ex vivo*, oxidative stress caused characteristic morphological changes and apoptosis of CE, suggestive of findings that characterize FECD *in vivo*. Together, these data suggest that suboptimal nuclear factor erythroid 2-related factor 2-regulated defenses may account for oxidant-antioxidant imbalance in FECD, which in turn leads to oxidative DNA damage and apoptosis. This study provides evidence that oxidative stress plays a key role in FECD pathogenesis. *(Am J Pathol 2010, 177:2278–2289; DOI: 10.2353/ajpath.2010.100279)*

Corneal endothelium (CE) is a monolayer of cells situated in the anterior chamber surface of the cornea; its primary function is to maintain the cornea in a state of deturgescence through sodium-activated ATPase pumping of water, thus, transparency. Fuchs endothelial corneal dystrophy (FECD) is the most common cause of endogenous corneal endothelial degeneration and is characterized by alterations in corneal endothelial cell morphology, progressive loss of CE cells, and concomitant accumulation of extracellular deposits in the basement membrane that eventually lead to corneal edema and opacity.[1]

Because CE does not divide *in vivo*, loss of endothelial cells seen in FECD is permanent. Corneal transplantation is the only treatment modality that can restore lost vision—rendering FECD the second most common cause of corneal transplants performed on the elderly (>60 years old) in the United States.[2] Lack of knowledge of the mechanism of CE degeneration in FECD precludes the development of pharmacotherapeutics for this common and blinding condition.

FECD has been termed a disorder of aging; it is a bilateral and slowly progressive disorder, typically appearing after the age of 60 years. FECD is usually a sporadic condition, but it can be inherited as an autosomal dominant trait.[3–5] FECD is characterized by endothelial cell apoptosis,[6,7] endothelial cell morphological changes, and concomitant extracellular matrix deposition in the form of mound-shaped excrescences, termed guttae. The loss of CE cells and the formation of guttae start in the central cornea and spread toward the periphery. The number of endothelial cells remaining in the cornea is inversely proportional to the number of guttae excrescences.[8] As the disease progresses, endothelial cell loss is accompanied by the thinning, stretching, and enlargement of neighboring CE cells as well as the loss of their

Supported by NEI K12 EY016335 (U.V.J.) and RO1 EY020581 from National Institute of Health.

U.V.J. and M.S.B. contributed equally to this work.

Accepted for publication July 6, 2010.

None of the authors disclosed any relevant financial relationships.

Current address of M.S.B.: Henry Ford Hospital, Detroit, MI.

Address reprint requests to Ula V. Jurkunas, M.D., Massachusetts Eye and Ear Infirmary, 243 Charles St, Boston, MA 02114; E-mail: ula_jurkunas@meei.harvard.edu.

hexagonal shape. Clinically, the endothelial morphological changes in FECD are denoted *polymegethism*, a variation in cell size, and *pleomorphism*, a variation in cell shape.

The putative role of oxidative stress in the pathogenesis of FECD has been proposed,[9,10] but little direct data on its role have been reported. CE is especially prone to oxidative stress due to its lifelong exposure to light (the cornea is in the direct light path to the retina), high oxygen demand from exuberant metabolic activity (it has to continually pump ions by Na^+K^+ATPases), and postmitotic arrest. Proteomic analysis of corneal endothelium taken from patients with FECD and age-matched normal controls has revealed decreased expression of peroxiredoxins (PRDXs), thioredoxin-dependent antioxidants that convert hydrogen peroxide (H_2O_2) to water.[11] In addition, increased levels of advanced glycation end products, nonenzymatically glycated proteins known to be associated with increased cellular oxidative stress, and their receptors, have been detected in FECD CE and Descemet's membrane compared with normal controls.[9] To date, the hypothesis that chronic oxidative stress causes molecular and cellular damage in susceptible human CE cells, which in turn leads to the pathological and clinical findings of FECD, has been hindered because no clear demonstration of oxidative cellular damage has been shown in FECD-affected endothelial cells. Yet, reports that show ultrastructural signs of "stress" with abundance of degenerated mitochondria, suggest that the mitochondria might be specific targets of oxidant-induced macromolecular damage in susceptible FECD CE cells.[12,13]

In this study, we sought to determine whether FECD is associated with oxidant-antioxidant imbalance, and if so, whether oxidant-induced DNA damage (specifically mitochondrial DNA damage) is present in diseased endothelium. We performed antioxidant gene profiling, comparing FECD CE with normal, and detected a decreased antioxidant defense system in FECD. Since the underexpressed antioxidants were found to have a common promoter region, the antioxidant response element (ARE), we investigated levels of ARE-binding transcription factors, nuclear factor erythroid 2-related factor-1 and -2 (Nrf1 and Nrf2, respectively) in FECD and normal CE. These transcription factors heterodimerize with small Maf proteins, bind ARE sequence, and cause coordinated up-regulation of antioxidant and xenobiotic-metabolizing enzyme genes during oxidative stress.[14–16]

We present three main lines of evidence that oxidative stress is the inciting factor of the pathophysiological processes seen in FECD: (1) There is an oxidant-antioxidant imbalance seen in FECD as compared with normal CE. (2) There is an accumulation of oxidized DNA lesions in FECD CE as compared with normal subjects. (3) Oxidative stress *in vitro* induces the characteristic morphological changes and apoptosis in CE seen in FECD. The correlation between oxidative damage and apoptosis in FECD CE provides key evidence in the role of oxidative stress in the pathogenesis of this age-related, chronic, corneal condition.

Table 1. Donor Information

	FECD	Normal	PBK
Average age*	68 ± 10	67 ± 7	67 ± 22
Sex (female/male)	27/7	23/10	2/2

*Average age in years with standard deviation shown.

Materials and Methods

Human Tissue

This study was conducted according to the tenets of the Declaration of Helsinki and was approved by the Massachusetts Eye and Ear Institutional Review Board. After surgical removal, one-third of the FECD and pseudophakic bullous keratopathy (PBK) corneal button was used for histopathological confirmation of the diagnosis and two-thirds was used for the study, and immediately stored in corneal storage medium (Optisol-GS; Bausch & Lomb, Tampa, FL) at 4°C. Fresh normal human corneal buttons from National Disease Research Interchange, Philadelphia, PA and Tissue Banks International, Baltimore, MD were used as controls. We used previously published criteria for donor tissue suitability.[17] Table 1 presents information regarding the tissue samples used. Normal donors were sex and decade matched with FECD and PBK donors.

Human Corneal Endothelial Cell Culture

An immortalized adult human corneal endothelial cell line (HCECi), previously established by SV40-transfection, was kindly provided by K. Engelmann (Department of Ophthalmology, University of Hamburg, Hamburg, Germany).[18] Cells were grown in T25 culture flasks in cell growth medium containing 8% fetal bovine serum. The culture medium of subconfluent cells was replaced with serum-free medium (OptiMEM-1; Invitrogen-Life Technologies, Carlsbad, CA) alone or supplemented with H_2O_2 (200 μmol/L) and incubated for 2 hours at 37°C. At the end of the treatment, cell viability was evaluated by trypan blue staining.

PCR Arrays

Under a dissecting microscope Descemet's membrane, along with the CE cell layer, was dissected from the stroma of corneal buttons. Total RNA was extracted from normal and FECD samples by using the RNeasy Micro kit (Qiagen, Valencia, CA). cDNA was prepared with the RT^2 First Strand Kit (SABiosciences, Frederick, MD) and loaded on the Human Oxidative Stress and Antioxidant Defense RT^2 Profiler PCR Array (SABiosciences). The PCR arrays were run on the ABI Prism 7900 HT (Applied Biosystems, Carlsbad, CA) sequence detection system. Dissociation curves showed specificity of the amplified product, except for one gene, the neutrophil cytosolic factor 1, which was excluded from the study. The average expression of the housekeeping genes β_2-microglobulin (B2M), ribosomal protein L13a, and β-actin was used for normalization. Data analysis was performed on a data analysis template provided by

SABiosciences. The comparative Ct method was used to calculate the mRNA fold-change in FECD CE relative to normal.

Identification of ARE Consensus Sequences

The National Center for Biotechnology Information sequences of genes that were more than twofold up- or down-regulated in FECD compared with normal were retrieved. Using Human BLAT, BLAST like alignment tool, a search for the consensus ARE core sequence (A/G TGACNNN GC) was carried out up to 5000 bp upstream of the transcription start site.[19] Complement sequences were also searched.

Western Blot Analysis

Under a dissecting microscope, Descemet's membrane, along with the CE cell layer, was dissected from the stroma of corneal buttons. Whole cell extracts were solubilized in protein extraction buffer ER3 (Bio-Rad, Hercules, CA) and 1 mmol/L tributyl phosphine and used for Western blot analysis. Western blot experiments were conducted as previously described.[11] Blots were incubated overnight with rabbit polyclonal anti-Nrf2 (1:100; Santa Cruz Biotechnology, Santa Cruz, CA), followed by incubation with horseradish peroxidase-conjugated secondary antibody. Mouse anti-β-actin (1:6000; Sigma Aldrich, St. Louis, MO) was used to normalize protein loading. Proteins were detected with an enhanced chemiluminescence detection kit (SuperSignal). Densitometry was performed with Kodak Digital Science 1D software.

Quantitative Analysis of 8-hydroxy-2′-deoxyguanosine

DNA was extracted from normal and FECD CE, and from H_2O_2-treated and nontreated HCECi by using QIAamp DNA Micro Kit (Qiagen) and eluted in distilled water. The DNA concentration of each sample was measured with the Nanodrop ND-1000 (Thermo Scientific, Waltham, MA). The DNA was digested with nuclease P1 (USBiological, Marblehead, MA) then treated with alkaline phosphatase (Roche, Indianapolis, IN), and filtered through the Microcon YM-10 ultrafiltration membrane (Millipore, Billerica, MA). The content of 8-hydroxy-2′-deoxyguanosine (8-OHdG) in each sample was determined by using the highly sensitive 8-OHdG enzyme-linked immunosorbent assay (ELISA) kit (Northwest Life Sciences Specialties LLC, Vancouver, WA). To normalize between samples, the 8-OHdG content of each sample was divided by the amount of DNA loaded, in nanograms.

Real-Time PCR

Total RNA was isolated from normal and FECD CE samples and from H_2O_2-treated and nontreated HCECi with the RNeasy Micro Kit (Qiagen). Reverse transcription was performed by using a commercially available kit (Promega, Madison, WI). TaqMan primers and probes for Nrf2, Nrf1, heme oxygenase-1 (HO-1), and for the endogenous control B2M were obtained from Applied Biosystems. Real-time PCR reactions were run on an ABI Prism 7500 HT Sequence Detection System (Applied Biosystems). For data analysis, the comparative Ct method was performed as previously established.[20]

Corneal Whole Mount Assays

Eight- to 12-week-old male BALB/c and C57BL/6 (from Taconic Farms, Germantown, NY, and our own breeding facility) were used for corneal whole mount assays. All protocols were approved by the Schepens Eye Research Institute Animal Care and Use Committee, and all animals were treated according to the Association for Research in Vision and Ophthalmology Statement for the Use of Animals in Ophthalmic and Vision Research. Whole mount corneas, endothelial cell side up, dissected from mice, were stored in serum-free Dulbecco's modified Eagle's medium (DMEM) and subjected to various concentrations of H_2O_2 (0 to 100 μmol/L) for variable time periods (30 minutes to 12 hours) at 37°C. Control corneal buttons were incubated in DMEM only at 37°C for 0 to 12 hours.

Immunocytochemistry

Immunocytochemistry was performed as previously described.[21] For mitochondrial staining, normal, FECD, and PBK corneas were incubated in culture medium containing 100 nmol/L MitoTracker Red CMXRos (Molecular Probes, Carlsbad, CA) for 30 minutes at 37°C, then fixed with 3.7% formaldehyde. After permeabilization, corneas were incubated with goat anti-8-OHdG (1:200; Millipore) followed by incubation with fluorescein isothiocyanate-conjugated donkey anti-goat IgG (Jackson ImmunoResearch, West Grove, PA) diluted at 1:200. Nuclei were stained with TO-PRO-3 iodide (Molecular Probes). For all other studies, tissues were fixed with 70% ethanol for 20 minutes. After permeabilization, tissues were incubated with goat anti-8-OHdG (1:200; Millipore) in 5% donkey serum (Jackson ImmunoResearch) or rabbit anti-Nrf2 (1:200) in 4% bovine serum albumin followed by incubation with appropriate secondary antibody and TO-PRO-3 iodide. After three 10-minute washes, terminal deoxynucleotidyl transferase-mediated dUTP nick-end labeling (TUNEL) assay (In Situ Cell Death Detection Kit; Roche Diagnostics GmbH, Indianapolis, IN) was performed according to manufacturers' instructions. For the whole mount assays, corneal endothelial tight junctions were detected by rabbit anti-zonula occludens-1 (anti-ZO-1) antibody (1:300; Invitrogen). Apoptosis was detected by using annexin-V-fluorescein isothiocyanate (1:20; Bioscience, San Jose, CA), propidium iodide (1:200; Invitrogen), and TUNEL assay (In Situ Cell Death Detection Kit; Roche Diagnostics GmbH) according to the manufacturers' instructions. Digital images were obtained by using a spectral photometric confocal microscope (Leica DM6000S with LCS 1.3.1 software). CE cells were counted by using particle analysis plug in, and TUNEL-positive cells were counted by using cell counter plug-in

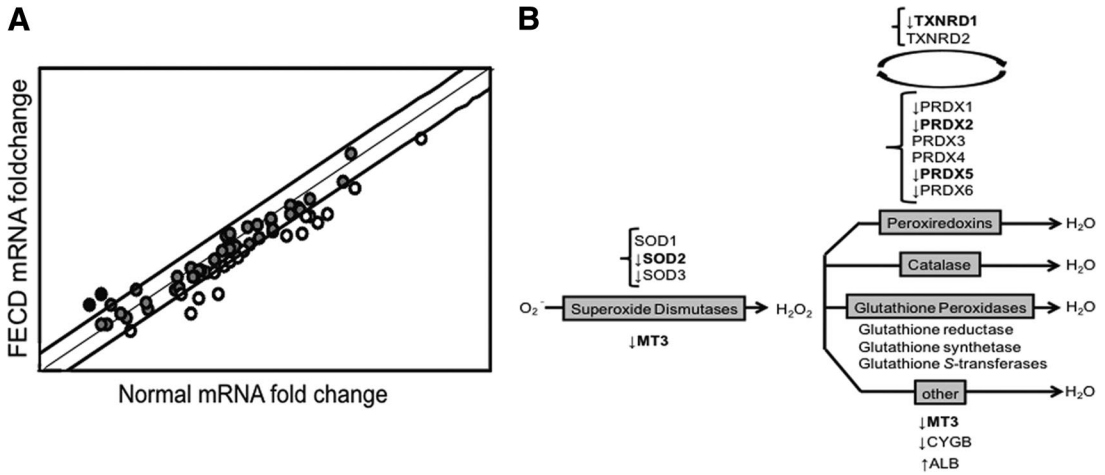

Figure 1. Relative expression of antioxidant and oxidative stress-related genes detected by PCR array in FECD and normal corneal endothelium. **A:** Scatter plot shows the distribution of the fold-changes in mRNAs between five normal and five FECD samples relative to the housekeeping genes B2M, ribosomal protein L13a, and β-actin. Bold lines represent a twofold change set as a threshold of up- and down-regulation. The middle line represents a fold-change of 1. Circles: black, more than twofold overexpressed genes; gray, gene expression less than twofold change; white, more than twofold change in underexpressed genes in FECD compared with normal. **B:** The data obtained from the PCR array are summarized in a scheme of the enzymatic antioxidant systems that reduce superoxide radical (O_2^-) and H_2O_2 to water. There are three forms of SOD, the main enzymes responsible for scavenging superoxide radical. PRDX5, catalase, and glutathione peroxidases are the primary enzymes responsible for scavenging H_2O_2. TXNRD1 catalyzes the regeneration of peroxiredoxins. Glutathione reductase, glutathione transferase, and glutathione synthetase are the components of the glutathione peroxidase system. The other antioxidant systems that scavenge H_2O_2 are MT3, cytoglobin (CYGB), and albumin (ALB). The **arrows** indicate which genes are overexpressed or underexpressed in FECD CE as compared with normal CE. **Boldfaced genes** had statistically significant fold changes in FECD CE compared with normal.

of the ImageJ software (NIH, Bethesda, MD). Cell density was calculated by dividing total number of cells by image area in mm^2. Fluorescently labeled 8-OHdG was quantified by dividing integrated fluorescence intensity (obtained by ImageJ) by the total number of cells.

Analysis of CE Cell Morphology

Images of corneal endothelium after staining with anti-ZO-1 were uploaded into Confoscan 4 (NIDEK Technologies, Padova, Italy) software, which performs automatic cell analysis. The software was used to detect the number of cell sides, the area of each cell, and endothelial cell density; polymegethism (variation in cell size) and pleomorphism (variation in cell shape) were then calculated.

Statistical Analysis

Data were analyzed with the statistical analysis software SPSS 16.0 (SPSS, Chicago, IL). Statistical analyses were performed by using a two-tailed unpaired Student's *t*-test, and one-way analysis of variance with significant differences between groups identified by using least–squares difference post hoc test. Results were expressed as mean ± SEM and considered significant for $P < 0.05$.

Results

Oxidant-Antioxidant Imbalance in FECD CE

Our previous study identified decreased levels of PRDX proteins in FECD CE.[11] The aim of the following experiments was to determine whether PRDX synthesis is the only antioxidant family affected in FECD, and whether there is alteration of expression or compensatory overexpression of other antioxidants in FECD CE. Human Oxidative Stress and Antioxidant Defense RT^2-PCR Arrays comparing native normal and FECD endothelial cells were used. The samples were age and sex matched (Table 1). A change in mRNA expression of more than twofold in FECD relative to normal was set as the cutoff value for considering a gene to be underexpressed or overexpressed. The PCR array included 84 oxidative stress-related genes, of which 61 (73%) had detectable expression in human corneal endothelium. Of the 61 genes detected, 18 transcripts (30%) were more than twofold underexpressed, and two (3%) were more than twofold overexpressed, as shown in the scatter plot (Figure 1A). Of the underexpressed genes, statistical significance ($P < 0.05$) was noted in five antioxidant genes: two genes related to apoptosis, two involved in cell signaling, and one involved in oxidative stress response (Table 2). The two overexpressed genes were albumin and neutrophil cytosolic factor 2.

A diagram depicting the main antioxidant enzyme systems responsible for reactive oxygen species (ROS) metabolism to water is shown in Figure 1B. The antioxidants found to be dysregulated in FECD are indicated with arrows. Transcriptional down-regulation of PRDX genes confirmed our previous findings.[11] In addition, down-regulation of thioredoxin reductase 1 (TXNRD1), a reductant necessary to replenish PRDX activity, and metallothionein 3 (MT3), a potent ROS scavenger, were noted. There was a decrease in two superoxide dismutase (SOD) isoforms, but only SOD2, a mitochondrial antioxidant, was down-regulated at a statistically significant level. We did not detect any compensatory overexpression of ubiquitous antioxidants such as catalase and

Table 2. Genes with More Than Twofold Down- or Up-Regulation in FECD Corneal Endothelium Relative to Normal as Detected by PCR Array

Gene description	Symbol	Fold regulation	*P*	ARE site in promoter
> Twofold down-regulated				
Antioxidant				
Metallothionein 3	***MT3***	**−5.65**	**0.02**	**x**
Superoxide dismutase 3, extracellular	*SOD3*	−5.37	0.10	x
Peroxiredoxin 2	***PRDX2***	**−4.30**	**0.04**	**x**
Peroxiredoxin 6	*PRDX6*	−3.29	0.06	x
Peroxiredoxin 5	***PRDX5***	**−3.05**	**0.01**	**x**
Superoxide dismutase 2, mitochondrial	***SOD2***	**−2.65**	**0.00**	**x**
Cytoglobin	*CYGB*	−2.23	0.16	x
Thioredoxin reductase 1	***TXNRD1***	**−2.23**	**0.02**	**x**
Peroxiredoxin 1	*PRDX1*	−2.02	0.19	x
ROS metabolism				
Nitric oxide synthase 2A (inducible, hepatocytes)	*NOS2A*	−3.91	0.22	
Arachidonate 12-lipoxygenase	*ALOX12*	−2.31	0.40	
Apoptosis				
BCL2/adenovirus E1B 19 kd interacting protein 3	***BNIP3***	**−4.61**	**0.00**	**x**
Glyceraldehyde-3-phosphate dehydrogenase	***GAPDH***	**−2.61**	**0.03**	
Signaling in response to oxidative stress				
Dual specificity phosphatase 1	***DUSP1***	**−3.12**	**0.01**	**x**
Oxidative-stress responsive 1	***OXSR1***	**−2.18**	**0.03**	**x**
Serine/threonine kinase 25 (STE20 homolog, yeast)	*STK25*	−2.16	0.11	x
Other oxidative stress responsive genes				
Angiopoietin-like 7	***ANGPTL7***	**−4.74**	**0.02**	**x**
Selenoprotein P, plasma, 1	*SEPP1*	−2.03	0.07	x
> Twofold up-regulated				
Antioxidant				
Albumin	*ALB*	3.34	0.15	
ROS metabolism				
Neutrophil cytosolic factor 2	***NCF2***	**3.48**	**0.02**	**x**

x, gene that has the ARE consensus sequence in its promoter sequence. Note: Bold-faced genes have statistically significant fold changes in FECD CE compared with normal.

glutathione peroxidases, or any other antioxidants involved in ROS scavenging.

To determine whether there is a common transcriptional regulation of the underexpressed antioxidants in FECD, a computer-based search for ARE (A/G TGACNNN GC)[19] in the promoter region of the genes, up to 5 kb upstream, was carried out. Fifteen out of 18 down-regulated genes (above the twofold cutoff) in FECD had a perfectly matched ARE sequence in the proximal promoter regions (Table 2).

The transcription factor Nrf2 is known to bind the ARE sequence and cause a coordinated up-regulation of antioxidant and xenobiotic-metabolizing enzyme genes during oxidative stress.[14,15] To examine the involvement of the Nrf2 transcription factor in FECD, we compared the levels of Nrf2 between normal and FECD CE. We detected a 5.4-fold decrease ($P = 0.03$) in Nrf2 protein level in FECD CE as compared with normal controls (Figure 2, A and B). In addition to a decreased production of Nrf2 protein, we detected a notable depletion in the expression of one of the major Nrf2-regulated antioxidant genes, HO-1[22] (Figure 2C) in FECD specimens as compared with normal controls ($P = 0.04$). Conversely, we did not detect a difference in Nrf1 expression between normal and FECD endothelium (Figure 2D). The immunocytochemical analysis detected that both FECD and normal samples show predominantly cytoplasmic distribution of Nrf2 (Figure 2E).

Increased Oxidative DNA Damage in FECD CE

To determine whether alterations in the antioxidant gene profile are accompanied by oxidant-mediated injury to the cell, levels of oxidative DNA damage in FECD endothelium were assayed. Accumulation of oxidized DNA is characteristic of ROS-induced molecular damage during aging and in pathological conditions that are linked to oxidative stress.[23–26] One of the major DNA base lesions is 8-OHdG.[27] A competitive ELISA was used to compare 8-OHdG levels between FECD and normal corneal endothelium. Figure 3A shows the average concentration of 8-OHdG normalized to the amount of DNA loaded in patients with FECD and normal controls. The FECD group had 2.17E-03 ± 6.01E-04 ng/ml 8-OHdG per ng of DNA, and the normal group 2.90E-04 ± 3.71E-05 ng/ml. Thus, the average level of 8-OHdG in FECD was 7.5-fold higher than in normal samples ($P = 0.006$). These results indicate that oxidative DNA damage is increased in FECD CE compared with age- and sex-matched controls.

Colocalization of Oxidative DNA Damage and Mitochondria

To determine whether oxidative DNA damage was in mitochondria or nuclei, normal and FECD CE was labeled

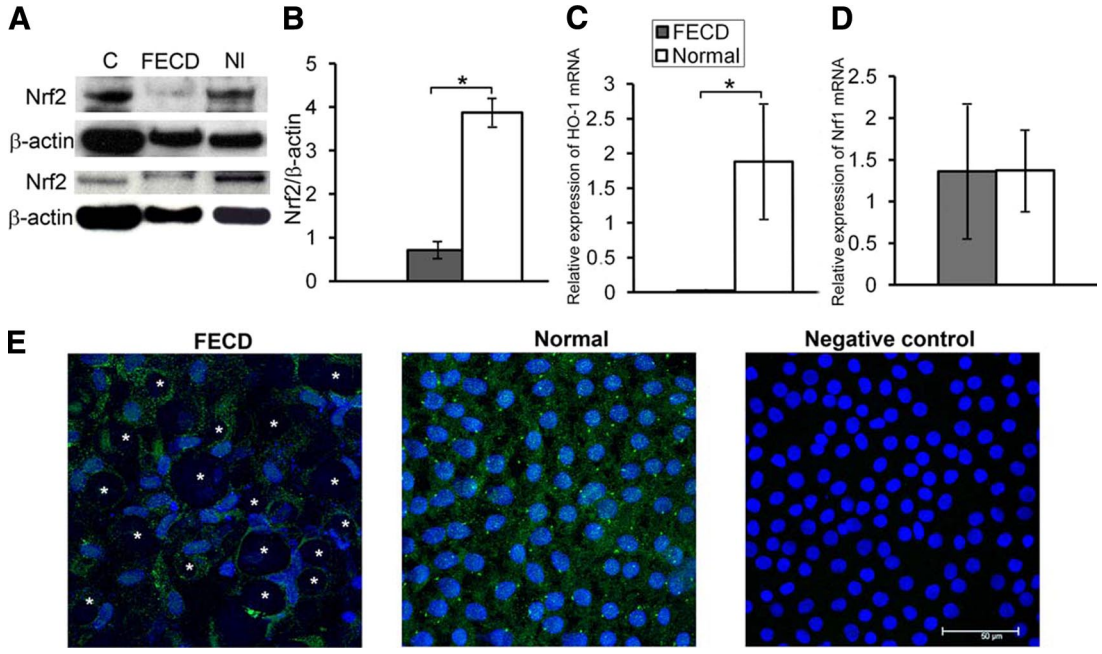

Figure 2. Decreased Nrf2 protein levels in FECD compared with normal endothelium. **A:** Western blot analysis of Nrf2 production in FECD and normal (Nl) corneal endothelial samples. Mouse kidney extract was used as a positive control (**C**). Bands were detected at the appropriate molecular weight of 57 kDa. β-actin was used for normalization of protein loading. **B:** Densitometric analysis of Nrf2 expression in CE. Data are means ± SEM of six FECD and six normal samples. Nrf2 protein levels were significantly decreased in FECD CE compared with normal controls; $^*P = 0.03$. **C:** Real-time PCR analysis showed a decrease in HO-1 expression in FECD compared with normal. Results were expressed as fold-changes and normalized to B2M mRNA expression from five FECD and normal samples. $^*P = 0.04$. **D:** Real-time PCR analysis did not detect a difference in Nrf1 expression between five FECD and five normal endothelial samples. **E:** Confocal images of corneal endothelium from FECD and normal patients were taken after immunolocalization of Nrf2 (green). TOPRO-3 was used for nuclei staining (blue). Negative control was incubated with secondary antibody only. Original magnification, ×400 with 2 zoom. **Asterisks** indicate the characteristic guttae of FECD CE; multiple guttae shown in the image.

with anti-8-OHdG antibody and MitoTracker, a mitochondrial selective probe that is taken up by mitochondria before cell fixation. For reference, *in vivo* confocal images of corneal endothelium from normal controls and patients with FECD are presented in Figure 3B. In normal endothelium, the mitochondria (red) are present throughout the cytoplasm, with greater aggregation around the nuclei (blue; Figure 3C). Minimal binding of the anti-8-OHdG antibody (green) is noted. In FECD CE, a characteristic rosette-type clustering of endothelial cells occurs around dark centers representing the guttae.[21] The total number of cells is diminished in FECD due to dystrophic degeneration (bottom row), as compared with normal tissue (top row). In diseased cells, the mitochondria-specific stain is present predominantly around the nuclei. There is significant binding of the anti-8-OHdG antibody primarily around the nuclei, which cluster around the guttae. Colocalization of 8-OHdG with mitochondria is clearly indicated by yellow fluorescence (Figure 3C). These findings provide evidence that it is primarily mitochondrial DNA that sustains oxidative damage in FECD-affected endothelium.

To assess whether molecular alterations seen in FECD tissue are induced by oxidative stress, immortalized HCECi were treated with H_2O_2. Cell viability was 96.9% in nontreated HCECi and 91.8% in H_2O_2-treated group. Following a 2-hour treatment with H_2O_2, there was a statistically significant decrease in Nrf2 transcription ($P = 0.004$) in treated cells compared with nontreated controls. The mean ± SEM relative expression of Nrf2 mRNA was (0.66 ± 0.02) and (1.00 ± 0.05), respectively (Figure 4A). Concomitantly, the level of 8-OHdG in cells exposed to H_2O_2 was twofold higher than in control cells ($P = 0.001$; Figure 4B). These *in vitro* studies suggest that oxidative stress causes a down-regulation of Nrf2 along with an increased amount of oxidative DNA damage *in vitro*, thus mimicking the changes seen in native diseased samples.

Colocalization of Oxidative DNA Damage and Apoptosis Is Specific to FECD

Another major reason for CE cell loss and development of edema in human cornea is PBK, a disease caused by iatrogenic damage to CE during surgery, mainly cataract extraction. To evaluate whether apoptotic cell death and oxidative damage are specific to FECD, level of apoptosis and oxidative damage were compared between normal, FECD, and PBK human specimens by labeling with TUNEL and anti-8-OHdG antibodies. Total number of CE cells per mm^2 was significantly lower in the specimens taken from FECD (933 ± 253; $P = 0.04$) and PBK (718 ± 313; $P = 0.04$) donors, as compared with normal controls (2079 ± 440; Figure 5, A and B). Significantly more TUNEL-labeled apoptotic cells were detected in FECD specimens compared with normal ($P = 0.017$) samples, whereas TUNEL binding was not statistically significant between normal and PBK ($P = 0.54$) samples (Figure 5, A and B). In addition, oxidative DNA damage, as indicated by 8-OHdG

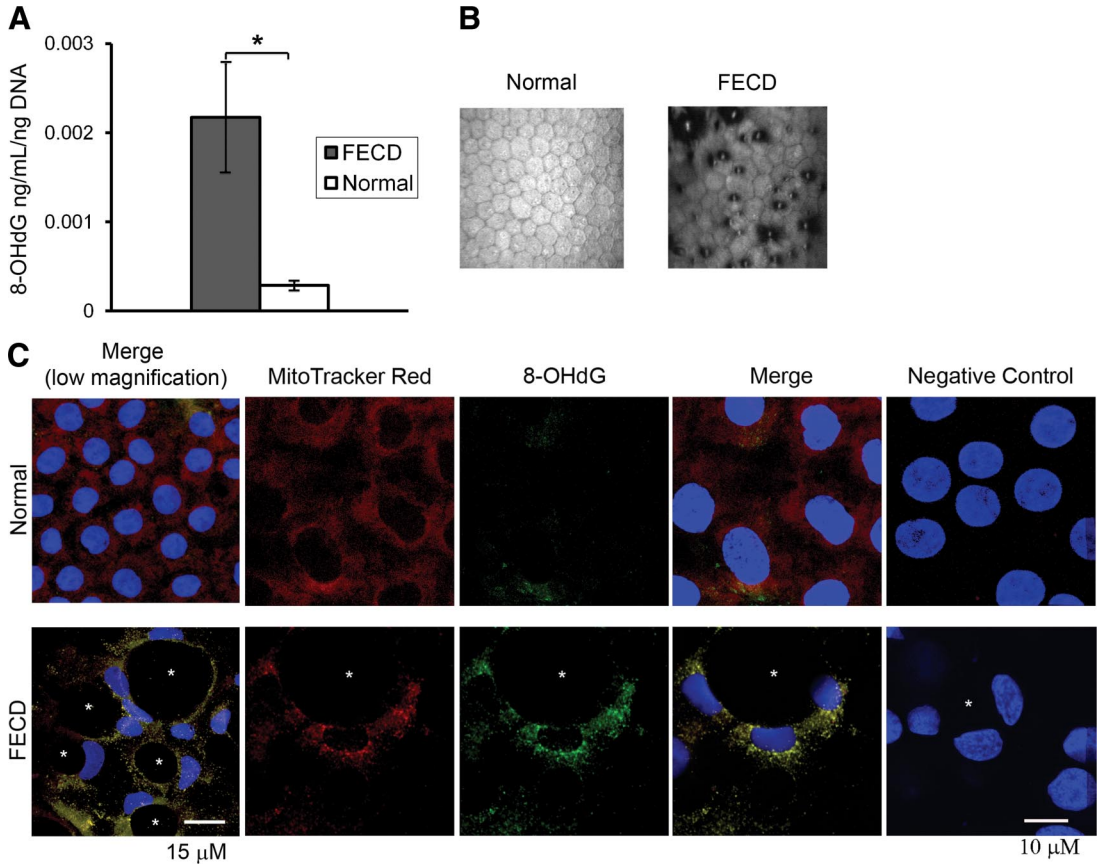

Figure 3. Increased oxidative DNA damage in FECD compared with normal CE and its colocalization with mitochondria. **A:** High-sensitivity ELISA was used to detect average concentration of 8-OHdG, an oxidative DNA damage marker, per nanogram DNA from patients with FECD and normal subjects. Data are means ± SEM of five FECD and five normal samples. The level of 8-OHdG in FECD CE was statistically significantly higher than in normal CE; $*P = 0.006$. **B:** *In vivo* confocal microscopy photographs of corneal endothelium from normal controls and patients with FECD. In FECD, the dark areas represent corneal guttae. **C:** Confocal images of normal (**top row**) and FECD CE (**bottom row**) in whole mounts of corneal tissue with endothelium side up. Representative images were taken after staining of mitochondria with MitoTracker Red, a mitochondrion-specific stain (red; **first column**), and immunolocalization of 8-OHdG (green; **second column**). Images of negative controls incubated with only secondary antibody are shown in the **right column**. TOPRO-3 was used for nuclei staining (blue). Overlay of the three channels shows colocalization of MitoTracker and 8-OHdG (**fourth column**) in FECD. **Asterisks** indicate the characteristic guttae of FECD CE. Original magnification, ×400 with 5 zoom (**first column**) and 8 zoom.

immunolocalization, was not detected in PBK corneas, while it colocalized with TUNEL-positive apoptotic cells in FECD specimens (Figure 5A). Densitometric analysis of confocal images detected increased 8-OHdG labeling in FECD as compared with normal controls ($P = 0.029$) but did not detect an increase in 8-OHdG labeling in PBK ($P = 0.644$) specimens (Figure 5C).

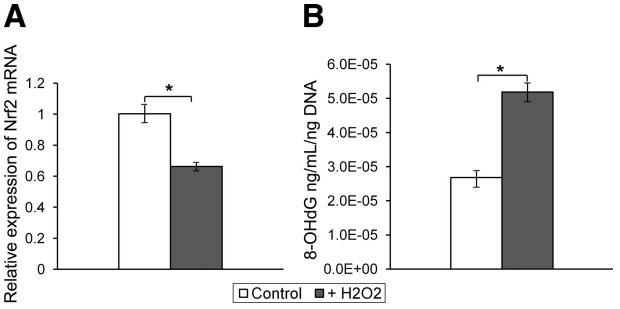

Figure 4. Effect of H_2O_2 treatment on the level of Nrf2 mRNA expression and oxidative DNA damage in HCECi. Corneal endothelial cells were treated with H_2O_2 (200 μmol/L) for 2 hours in three independent experiments. **A:** Real-time PCR analysis showed a decrease in Nrf2 expression after treatment with H_2O_2 ($+H_2O_2$) compared with nontreated HCECi (control). Results are expressed as fold-changes and normalized to B2M mRNA expression. **B:** High-sensitivity ELISA detected an increase in the average level of oxidized DNA (8-OHdG) in $+H_2O_2$-treated cells compared with control. Data are means ± SEM; $*P < 0.05$.

Oxidative Stress Induces CE Cell Polymegethism and Pleomorphism

To investigate the role of oxidative stress on CE cell morphological changes, denoted as polymegethism and pleomorphism, that are seen in FECD clinically (Figure 6A), excised mouse corneas with endothelial side up were treated with H_2O_2 in the corneal whole mount assay. CE tight junctions were labeled with anti-ZO-1 antibody, and Confoscan 4 software was used to determine endothelial cell density and morphological changes due to oxidative stress *ex vivo* (Figure 6B). Normal mouse CE cell density per mm^2 was 2943 ± 221, coefficient of variation (measure of polymegethism) 19.6% ± 0.83, and percentage of hexagonal cells (measure of pleomorphism) was 56.6% ± 2.4 (Figure 6C). A statistically significant change in polymegethism was induced after 50 μmol/L ($P < 0.001$) and 100 μmol/L ($P < 0.001$)

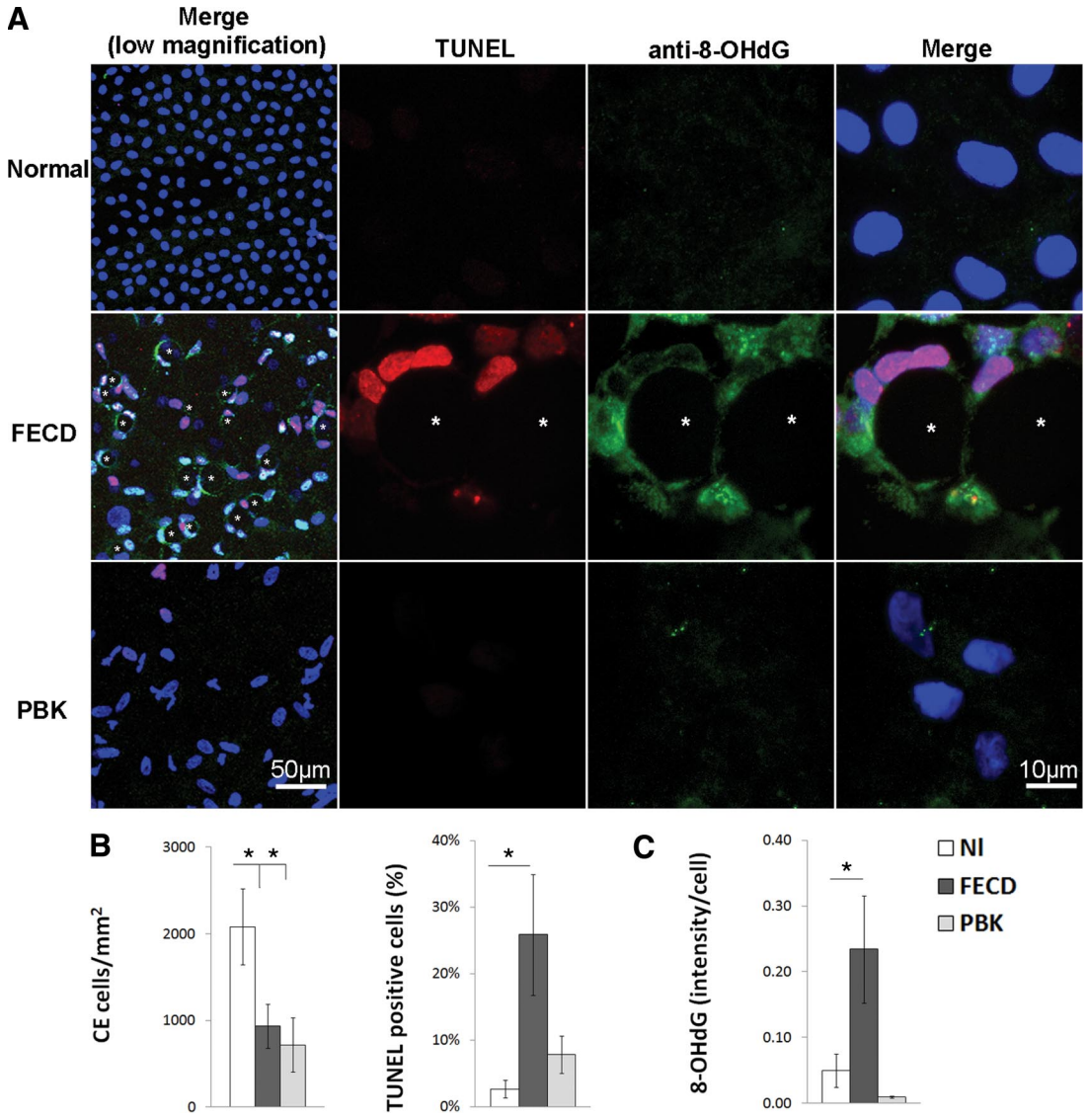

Figure 5. Colocalization of apoptosis and oxidative DNA damage in FECD compared with normal and PBK specimens. **A:** Corneal endothelium attached to its native basement membrane from normal (**top**), FECD (**middle**), and PBK (**bottom**) donors was labeled with TUNEL (red), anti-8-OHdG (green), and TOPRO-3 (blue). Colocalization of TUNEL and anti-8-OHdG antibodies is detected in CE cells from FECD specimens but not from PBK and normal corneas. **Asterisks** indicate the characteristic guttae of FECD CE. Original magnifications, ×600 and ×400 with 8 zoom. **B:** Corneal endothelial cell density is significantly lower in FECD and PBK specimens. The percentage of TUNEL-positive cells is higher in FECD. **C:** Densitometric analysis of CE labeled with anti-8-OHdG antibody indicates a significant increase in oxidative damage in FECD but not PBK compared with normal controls. Data are means ± SEM of four of each normal, FECD, and PBK samples; $^*P < 0.05$ compared with normal CE.

treatments, whereas the percentage of hexagonal cells declined significantly after 100 μmol/L treatments ($P = 0.007$; Figure 6C). Therefore, H_2O_2 treatments induced a dose-dependent increase in polymegethism and an increase in pleomorphism (Figure 6C). There was no statistically significant effect of pro-oxidant treatments on CE cell density as measured by ZO-1 labeling.

Corneal Endothelial Cell Apoptosis and Loss of Mitochondrial Membrane Potential due to Oxidative Stress Ex Vivo

Apoptotic cell death has been demonstrated in FECD endothelium[6,7] (Figure 5). To evaluate the role of oxidative stress on CE cell apoptosis in *ex vivo* corneal organ culture, where endothelium is attached to its native basement membrane, excised mouse corneas were treated with low-dose (1 μmol/L) H_2O_2. Labeling of exposed phosphatidylserine on the outer phospholipid leaflet of the plasma membrane by annexin-V antibodies enabled visualization of the time-dependent onset of CE cell early apoptosis (Figure 7, A, B, and C). Approximately 5% and 11% of CE cells exhibited early apoptosis as detected by annexin-V-positive and PI (propidium iodide)-negative staining at 60 minutes ($P < 0.01$) and 90 minutes ($P < 0.01$), respectively (Figure 7E). Late apoptosis, as detected by annexin-V-positive and PI-positive staining, was identified at 120 minutes ($P < 0.01$; Figure 7, D and E). Necrosis, detected by PI staining without annexin-V labeling, constituted a very minimal component of CE

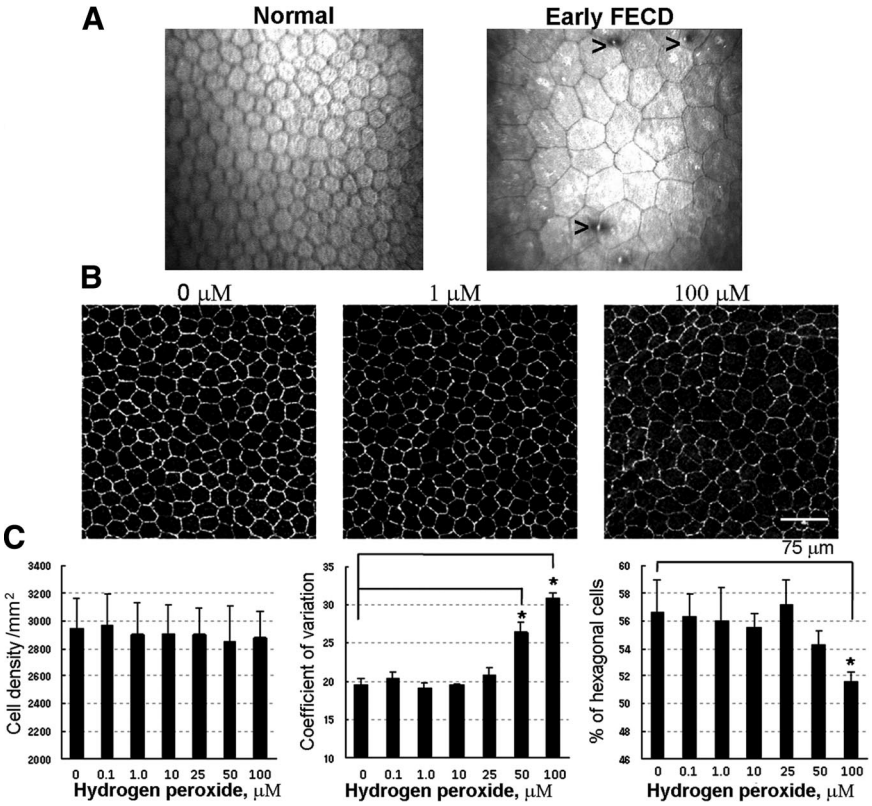

Figure 6. Effect of H_2O_2 treatment on CE morphology. **A:** *In vivo* confocal microscopy photographs of corneal endothelium from normal controls and patients with FECD. Normal endothelium exhibits regularly shaped hexagonal CE cells. In FECD, the CE cell mosaic is interrupted by guttae (**arrowheads**) and exhibits variable size (polymegethism) and variable shape (pleomorphism). **B:** Mice corneal buttons were treated with H_2O_2-DMEM (0 to 100 μmol/L) for 30 minutes. Confocal images of the whole mount corneas with CE cell junctions detected by ZO-1 (white) localization. **C:** Automated cell analysis did not detect a change in CE cell density with increasing H_2O_2 concentrations, but the level of polymegethism (measured by coefficient of variation) and pleomorphism (measured by the number of hexagonal cells) was significantly altered after treatment with H_2O_2 at 50 μmol/L or greater concentrations. Data are means ± SD and are representative of four independent experiments; $^*P < 0.05$, compared with untreated controls.

death due to low-grade oxidative stress. Corneal buttons incubated for the same time periods in only DMEM did not exhibit a statistically significant increase in apoptotic cell death.

To investigate whether there is an alteration of CE cell mitochondrial viability due to oxidative stress (H_2O_2, 1 μmol/L), CE cells *ex vivo* were labeled with MitoTracker CMXRos probe. Mitochondria showed dense staining

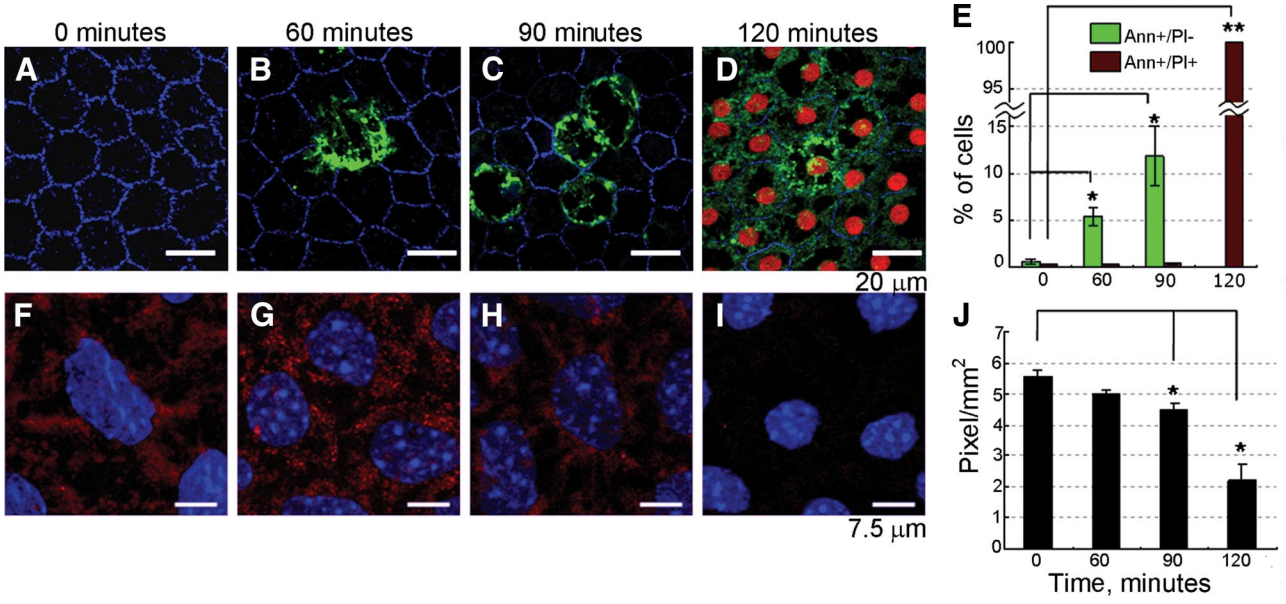

Figure 7. The effect of H_2O_2 on CE apoptosis and mitochondrial membrane potential *ex vivo*. Confocal images of whole mounts of mice corneal endothelium with detection of early apoptosis by annexin-V (green; Ann^+/PI^-) and late apoptosis by annexin-V and propidium iodide (red; Ann^+/PI^+). Endothelial cell junctions were detected by ZO-1 labeling (blue; **A–D**). Low-dose H_2O_2 (1 μmol/L, 37°C) induced early apoptosis after 60 minutes (**B**) and 90 minutes (**C**), and late apoptosis after 2 hours (**D** and **E**) compared with controls (**A**). Concurrent changes in staining with MitoTracker Red (red) were present at 60 minutes (**G**), 90 minutes (**H**), and 2 hours after the treatment (**I** and **J**). Cell nuclei were detected by TO-PRO-3 (blue) stain (**F–I**). Controls were incubated in DMEM only at 37°C for 0 to 12 hours, and no significant changes were detected (**A** and **F**). Results shown in **E** and **J** are means ± SD and are representative of four independent experiments; $^*P < 0.05$, compared with untreated controls; $^*P < 0.01$, compared with untreated controls.

with MitoTracker in the untreated corneas (Figure 7F), whereas a decline in the mitochondrial density was identified after the 1-hour treatment (Figure 7G). A significant decrease in detectable mitochondrial staining was present after 90 minutes ($P < 0.01$; Figure 7H), and no detectable mitochondrial staining was noted after the 2-hour H_2O_2 treatment ($P < 0.01$; Figure 7I). There was a time-dependent loss of mitochondrial density due to low-grade oxidative stress (Figure 7J). The timing of initial decline in mitochondrial staining (between 60 and 90 minutes) correlated with early apoptotic changes. Late apoptosis (2 hours) correlated with the absence of mitochondria-specific dye uptake into CE and possibly complete loss of mitochondrial membrane potential.

Discussion

There is increasing evidence that supports the hypothesis that chronic oxidative stress contributes to cellular and molecular damage in susceptible human corneal endothelial cells, which in turn leads to the pathological findings of FECD. Corneal endothelial degeneration is known to occur via apoptosis in FECD.[6,7] One of the major inducers of cellular apoptosis is macromolecular damage due to oxidative stress.[28] Since corneal endothelium is arrested in a postmitotic state, it is susceptible to reactive oxygen species-induced apoptosis as a result of aging and oxidative stress,[29,30] similar to neurons in neurodegenerative conditions.[23,31] Our study demonstrates, for the first time, the presence of oxidative damage in FECD corneal endothelium and concomitant modulation of the antioxidant gene profile, supporting the hypothesis that oxidative stress is an important contributor to the corneal endothelial morphological changes, apoptosis, and subsequent degeneration in FECD.

Previously, proteomic analysis demonstrated a deficiency in PRDX antioxidants in FECD-affected corneal endothelium.[11] The PCR array presented herein, comparing native normal and FECD CE, detected transcriptional down-regulation of PRDX genes, thus confirming the proteomic data. In addition, the PCR array was performed to determine whether antioxidant genes other than PRDX were affected in FECD. We detected a decrease in other antioxidants, such as SOD2, MT3, and TXNRD1; the latter being involved in restoring reducing equivalents required for PRDX enzymatic activity (Figure 1B). Several genes involved in apoptosis and signaling in response to oxidative stress were also down-regulated, as shown in Table 2. Surprisingly, no compensatory increase in the level of antioxidants, such as catalase or glutathione peroxidases and/or transferases, was observed. Such generalized down-regulation (and lack of up-regulation) of antioxidants in FECD points to diminished transcriptional activation of the promoter sites common to cellular antioxidant defense, as discussed below.[32,33] Taken together, our results indicate that there is a generalized down-regulation of the oxidative stress-related genes, tipping the oxidant-antioxidant balance toward a pro-oxidant state in FECD.

It has been shown that, in response to oxidative stress, cells function to counteract the oxidant effects and restore redox balance by activating or silencing genes encoding defensive enzymes, transcription factors, stress-induced proteins, and apoptotic pathways.[24,34,35] In this study, we determined that the down-regulated antioxidants in FECD contain ARE in their proximal promoter regions. Based on studies of other cell types, it is known that activation of antioxidants such as PRDXs, TXNRDs, SODs, and MT3 is dependent on Nrf2 transcription factor via binding of the ARE.[15,36–39] We detected a decrease in Nrf2 protein level in FECD samples as compared with normal controls. In addition, a major Nrf2-regulated gene, HO-1, was significantly down-regulated in FECD as compared with normal samples. Even though Nrf1 and Nrf2 have a significant overlap in regulation of ARE-dependent genes, no change in Nrf1 expression was noted between FECD and normal CE. This is consistent with the fact that Nrf2 is mainly involved in transcriptional up-regulation of antioxidants in response to oxidative stress.[40–42] Such a decrease in Nrf2 protein level, along with evidence of Nrf2 antioxidant target decline in FECD, provides evidence that there is potential dysregulation of Nrf2-regulated constitutive expression of multiple antioxidants in FECD corneal endothelium.

Previous studies have shown that Nrf2-ARE-driven gene activation protects neuronal cells from H_2O_2-induced apoptosis.[32,38] Given the extensive oxidative DNA damage in FECD, we expected that Nrf2 would be up-regulated in FECD in response to oxidative injury. However, a decline in Nrf2 protein in FECD might suggest an aberrant Nrf2 response in the diseased cells. Similarly, studies have not detected Nrf2 activation in Alzheimer's disease brains despite evidence of oxidative stress in the neuronal cells.[43] In previous studies, Nrf2 deletion in mice demonstrated a direct link between the regulation of

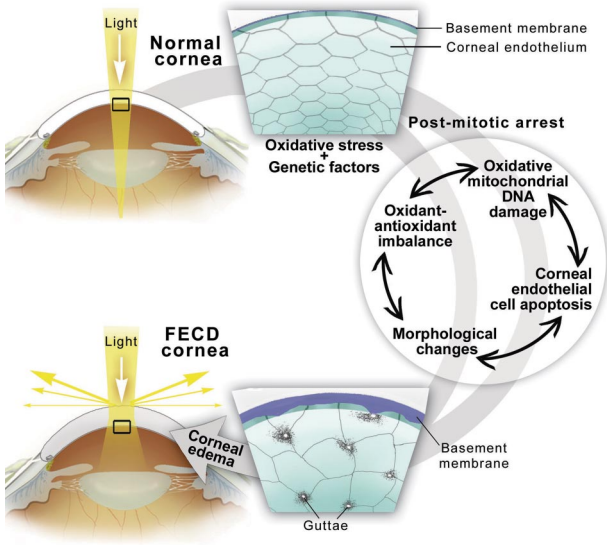

Figure 8. Diagram of the pathogenesis of FECD. Endogenous and exogenous oxidative stress combined with genetic factors and postmitotic arrest of CE may lead to corneal edema seen in FECD since it causes oxidant-antioxidant imbalance, oxidative mitochondrial DNA damage, apoptosis, and CE morphological changes.

antioxidant genes and oxidative stress-induced tissue destruction[44]; it is not clear if these mice have associated corneal defects. However, we confirmed, in an *in vitro* model using corneal endothelial cells, that H_2O_2 can cause concomitant down-regulation of Nrf2 and an increase in DNA oxidative damage. Therefore, the dysregulated Nrf2-controlled pathway is of critical relevance to understanding the cellular and molecular mechanisms that cause endothelial cell oxidative damage and, potentially, apoptosis in FECD. Targeting Nrf2, which up-regulates a wide range of antioxidants and confers cytoprotection[38,41,45,46] in other oxidative stress-related disorders, could be an attractive pharmacological strategy for treating corneal endothelium in the future.

Oxidative stress in a cell leads to DNA damage. We found increased levels of 8-OHdG, a marker of oxidative damage to DNA,[47–49] in FECD CE as compared with age-matched controls. The finding of elevated levels of oxidized guanosine base in FECD is particularly relevant and important, and, for the first time, places FECD in the category of oxidative stress-related disorders. Furthermore, consistent with the other oxidative stress-related degenerative disorders, such as Alzheimer's disease, age-related macular degeneration, and Parkinson's disease,[26,50,51] our study detected that mtDNA is the primary target of oxidative damage in FECD. mtDNA is particularly susceptible to oxidative damage due to several factors; it is located close to the ROS-generating respiratory chain, it is not covered by histones, and it lacks a strong repair system compared with that of nuclear DNA.[52–54] Previous studies have revealed that there are decreased numbers of mitochondria in FECD endothelium, and that activity of cytochrome oxidase, the major respiratory chain enzyme, is decreased in the central area of FECD corneal buttons.[55] Based on our studies, these findings are consistent with oxidative stress-induced mtDNA damage that could lead to loss of integrity of inner mitochondrial membrane potential and apoptotic cell death.

The key characteristic features of FECD are apoptotic cell death and aberrant extracellular matrix deposition that manifests in disruption of the hexagonal CE cell mosaic. Our studies on native FECD specimens correlate apoptotic cell death and oxidative damage. Importantly, we show that these findings are specific to the dystrophic degeneration and do not occur in PBK, a condition that also manifests in CE cell loss and corneal edema. Based on the studies on *ex vivo* corneas, oxidative stress induces morphological alterations in endothelial cell size and shape that mimic the changes seen in FECD. In addition, oxidative stress-induced CE cell loss of mitochondrial membrane potential correlated with the onset of early and late apoptosis in the *ex vivo* setting, thus pointing to a potential mechanism for endothelial cell loss in FECD. Based on the findings presented herein, we propose a schematic representation of the pathogenesis of FECD (Figure 8). The protein and gene profiling studies, along with the identification of the intracellular oxidative damage in the endothelium affected by the dystrophy, addresses the interaction of genetic factors (which are mostly unknown in FECD at this time) and environmental factors, thus enabling characterization of the pathogenic mechanisms that eventually lead to loss of CE cells and corneal edema.

In summary, our study demonstrates that there is down-regulation of ARE-driven antioxidant and oxidative stress-related gene expression, a decline in the levels of the major transcription factor known to regulate ARE-dependent antioxidants, and an increase in oxidative mtDNA damage in FECD. The suboptimal Nrf2-regulated antioxidant defense most likely contributes to the oxidant-antioxidant imbalance seen in FECD. Based on the findings of this study, oxidative stress directly associates with FECD pathogenesis and is a novel and attractive target for potential therapy development for this common ocular condition. The ability to prevent corneal endothelial cell loss in early as well as late stages of the disease by reversing oxidant-antioxidant imbalance would be highly relevant for generating therapies that either delay or bypass completely the need for corneal transplantation.

Acknowledgments

We thank all of the cornea surgeons and the Tissue Banks International for donating corneas; Dr. Ilene Gipson, Ph.D., (Schepens Eye Research Institute) for critical reading of the article; and Yuming Chen for technical support.

References

1. Wilson SE, Bourne WM: Fuchs' dystrophy. Cornea 1988, 7:2–18
2. Darlington JK, Adrean SD, Schwab IR: Trends of penetrating keratoplasty in the United States from 1980 to 2004. Ophthalmology 2006, 113:2171–2175
3. Cross HE, Maumenee AE, Cantolino SJ: Inheritance of Fuchs' endothelial dystrophy. Arch Ophthalmol 1971, 85:268–272
4. Krachmer JH, Purcell JJ, Jr., Young CW, Bucher KD: Corneal endothelial dystrophy: a study of 64 families. Arch Ophthalmol 1978, 96:2036–2039
5. Vithana EN, Morgan PE, Ramprasad V, Tan DT, Yong VH, Venkataraman D, Venkatraman A, Yam GH, Nagasamy S, Law RW, Rajagopal R, Pang CP, Kumaramanickevel G, Casey JR, Aung T: SLC4A11 mutations in Fuchs endothelial corneal dystrophy. Hum Mol Genet 2008, 17:656–666
6. Borderie VM, Baudrimont M, Vallee A, Ereau TL, Gray F, Laroche L: Corneal endothelial cell apoptosis in patients with Fuchs' dystrophy. Invest Ophthalmol Vis Sci 2000, 41:2501–2505
7. Li QJ, Ashraf MF, Shen DF, Green WR, Stark WJ, Chan CC, O'Brien TP: The role of apoptosis in the pathogenesis of Fuchs endothelial dystrophy of the cornea. Arch Ophthalmol 2001, 119:1597–1604
8. Waring GO, 3rd, Bourne WM, Edelhauser HF, Kenyon KR: The corneal endothelium: normal and pathologic structure and function. Ophthalmology 1982, 89:531–590
9. Wang Z, Handa JT, Green WR, Stark WJ, Weinberg RS, Jun AS: Advanced glycation end products and receptors in Fuchs' dystrophy corneas undergoing Descemet's stripping with endothelial keratoplasty. Ophthalmology 2007, 114:1453–1460
10. Buddi R, Lin B, Atilano SR, Zorapapel NC, Kenney MC, Brown DJ: Evidence of oxidative stress in human corneal diseases. J Histochem Cytochem 2002, 50:341–351
11. Jurkunas UV, Rawe I, Bitar MS, Zhu C, Harris DL, Colby K, Joyce NC: Decreased expression of peroxiredoxins in Fuchs' endothelial dystrophy. Invest Ophthalmol Vis Sci 2008, 49:2956–2963
12. Borboli S, Colby K: Mechanisms of disease: fuchs' endothelial dystrophy. Ophthalmol Clin North Am 2002, 15:17–25
13. Zhang C, Bell WR, Sundin OH, De La Cruz Z, Stark WJ, Green WR, Gottsch JD: Immunohistochemistry and electron microscopy of early-

onset fuchs corneal dystrophy in three cases with the same L450W COL8A2 mutation. Trans Am Ophthalmol Soc 2006, 104:85–97
14. Ishii T, Itoh K, Takahashi S, Sato H, Yanagawa T, Katoh Y, Bannai S, Yamamoto M: Transcription factor Nrf2 coordinately regulates a group of oxidative stress-inducible genes in macrophages. J Biol Chem 2000, 275:16023–16029
15. Shih AY, Johnson DA, Wong G, Kraft AD, Jiang L, Erb H, Johnson JA, Murphy TH: Coordinate regulation of glutathione biosynthesis and release by Nrf2-expressing glia potently protects neurons from oxidative stress. J Neurosci 2003, 23:3394–3406
16. Blank V: Small Maf proteins in mammalian gene control: mere dimerization partners or dynamic transcriptional regulators? J Mol Biol 2008, 376:913–925
17. Joyce NC, Zhu CC: Human corneal endothelial cell proliferation: potential for use in regenerative medicine. Cornea 2004, 23:S8–S19
18. Bednarz J, Teifel M, Friedl P, Engelmann K: Immortalization of human corneal endothelial cells using electroporation protocol optimized for human corneal endothelial and human retinal pigment epithelial cells. Acta Ophthalmol Scand 2000, 78:130–136
19. Rushmore TH, Morton MR, Pickett CB: The antioxidant responsive element: activation by oxidative stress and identification of the DNA consensus sequence required for functional activity. J Biol Chem 1991, 266:11632–11639
20. Jurkunas UV, Bitar M, Rawe I: Colocalization of increased transforming growth factor-beta-induced protein (TGFBIp) and Clusterin in Fuchs endothelial corneal dystrophy. Invest Ophthalmol Vis Sci 2009, 50:1129–1136
21. Jurkunas UV, Bitar MS, Rawe I, Harris DL, Colby K, Joyce NC: Increased clusterin expression in Fuchs' endothelial dystrophy. Invest Ophthalmol Vis Sci 2008, 49:2946–2955
22. Zhang J, Ohta T, Maruyama A, Hosoya T, Nishikawa K, Maher JM, Shibahara S, Itoh K, Yamamoto M: BRG1 interacts with Nrf2 to selectively mediate HO-1 induction in response to oxidative stress. Mol Cell Biol 2006, 26:7942–7952
23. Hamilton ML, Van Remmen H, Drake JA, Yang H, Guo ZM, Kewitt K, Walter CA, Richardson A: Does oxidative damage to DNA increase with age? Proc Natl Acad Sci USA 2001, 98:10469–10474
24. Lu T, Pan Y, Kao SY, Li C, Kohane I, Chan J, Yankner BA: Gene regulation and DNA damage in the ageing human brain. Nature 2004, 429:883–891
25. Nakabeppu Y, Tsuchimoto D, Yamaguchi H, Sakumi K: Oxidative damage in nucleic acids and Parkinson's disease. J Neurosci Res 2007, 85:919–934
26. Wang AL, Lukas TJ, Yuan M, Neufeld AH: Increased mitochondrial DNA damage and down-regulation of DNA repair enzymes in aged rodent retinal pigment epithelium and choroid. Mol Vis 2008, 14:644–651
27. Valavanidis A, Vlahoyianni T, Fiotakis K: Comparative study of the formation of oxidative damage marker 8-hydroxy-2′-deoxyguanosine (8-OHdG) adduct from the nucleoside 2′-deoxyguanosine by transition metals and suspensions of particulate matter in relation to metal content and redox reactivity. Free Radic Res 2005, 39:1071–1081
28. Ryter SW, Kim HP, Hoetzel A, Park JW, Nakahira K, Wang X, Choi AM: Mechanisms of cell death in oxidative stress. Antioxid Redox Signal 2007, 9:49–89
29. Cho KS, Lee EH, Choi JS, Joo CK: Reactive oxygen species-induced apoptosis and necrosis in bovine corneal endothelial cells. Invest Ophthalmol Vis Sci 1999, 40:911–919
30. Joyce NC, Zhu CC, Harris DL: Relationship among oxidative stress, DNA damage, and proliferative capacity in human corneal endothelium. Invest Ophthalmol Vis Sci 2009, 50:2116–2122
31. Simonian NA, Coyle JT: Oxidative stress in neurodegenerative diseases. Annu Rev Pharmacol Toxicol 1996, 36:83–106
32. Kraft AD, Johnson DA, Johnson JA: Nuclear factor E2-related factor 2-dependent antioxidant response element activation by tert-butylhydroquinone and sulforaphane occurring preferentially in astrocytes conditions neurons against oxidative insult. J Neurosci 2004, 24:1101–1112
33. Guzik TJ, Sadowski J, Guzik B, Jopek A, Kapelak B, Przybylowski P, Wierzbicki K, Korbut R, Harrison DG, Channon KM: Coronary artery superoxide production and nox isoform expression in human coronary artery disease. Arterioscler Thromb Vasc Biol 2006, 26:333–339
34. Hancock JT, Desikan R, Neill SJ: Role of reactive oxygen species in cell signalling pathways. Biochem Soc Trans 2001, 29:345–350
35. Thorpe GW, Fong CS, Alic N, Higgins VJ, Dawes IW: Cells have distinct mechanisms to maintain protection against different reactive oxygen species: oxidative-stress-response genes. Proc Natl Acad Sci USA 2004, 101:6564–6569
36. Lyakhovich VV, Vavilin VA, Zenkov NK, Menshchikova EB: Active defense under oxidative stress: the antioxidant responsive element. Biochemistry (Mosc) 2006, 71:962–974
37. Hwang YP, Kim HG, Han EH, Jeong HG: Metallothionein-III protects against 6-hydroxydopamine-induced oxidative stress by increasing expression of heme oxygenase-1 in a PI3K and ERK/Nrf2-dependent manner. Toxicol Appl Pharmacol 2008, 231:318–327
38. Li J, Johnson D, Calkins M, Wright L, Svendsen C, Johnson J: Stabilization of Nrf2 by tBHQ confers protection against oxidative stress-induced cell death in human neural stem cells. Toxicol Sci 2005, 83:313–328
39. Lee JM, Calkins MJ, Chan K, Kan YW, Johnson JA: Identification of the NF-E2-related factor-2-dependent genes conferring protection against oxidative stress in primary cortical astrocytes using oligonucleotide microarray analysis. J Biol Chem 2003, 278:12029–12038
40. Li N, Alam J, Venkatesan MI, Eiguren-Fernandez A, Schmitz D, Di Stefano E, Slaughter N, Killeen E, Wang X, Huang A, Wang M, Miguel AH, Cho A, Sioutas C, Nel AE: Nrf2 is a key transcription factor that regulates antioxidant defense in macrophages and epithelial cells: protecting against the proinflammatory and oxidizing effects of diesel exhaust chemicals. J Immunol 2004, 173:3467–3481
41. Lee JM, Li J, Johnson DA, Stein TD, Kraft AD, Calkins MJ, Jakel RJ, Johnson JA: Nrf2, a multi-organ protector? FASEB J 2005, 19:1061–1066
42. Chen W, Sun Z, Wang XJ, Jiang T, Huang Z, Fang D, Zhang DD: Direct interaction between Nrf2 and p21(Cip1/WAF1) upregulates the Nrf2-mediated antioxidant response. Mol Cell 2009, 34:663–673
43. Ramsey CP, Glass CA, Montgomery MB, Lindl KA, Ritson GP, Chia LA, Hamilton RL, Chu CT, Jordan-Sciutto KL: Expression of Nrf2 in neurodegenerative diseases. J Neuropathol Exp Neurol 2007, 66:75–85
44. Rangasamy T, Cho CY, Thimmulappa RK, Zhen L, Srisuma SS, Kensler TW, Yamamoto M, Petrache I, Tuder RM, Biswal S: Genetic ablation of Nrf2 enhances susceptibility to cigarette smoke-induced emphysema in mice. J Clin Invest 2004, 114:1248–1259
45. Chen PC, Vargas MR, Pani AK, Smeyne RJ, Johnson DA, Kan YW, Johnson JA: Nrf2-mediated neuroprotection in the MPTP mouse model of Parkinson's disease: Critical role for the astrocyte. Proc Natl Acad Sci USA 2009, 106:2933–2938
46. Xue M, Qian Q, Adaikalakoteswari A, Rabbani N, Babaei-Jadidi R, Thornalley PJ: Activation of NF-E2-related factor-2 reverses biochemical dysfunction of endothelial cells induced by hyperglycemia linked to vascular disease. Diabetes 2008, 57:2809–2817
47. Mecocci P, MacGarvey U, Kaufman AE, Koontz D, Shoffner JM, Wallace DC, Beal MF: Oxidative damage to mitochondrial DNA shows marked age-dependent increases in human brain. Ann Neurol 1993, 34:609–616
48. Arnheim N, Cortopassi G: Deleterious mitochondrial DNA mutations accumulate in aging human tissues. Mutat Res 1992, 275:157–167
49. Joyce NC, Harris DL, Zieske JD: Mitotic inhibition of corneal endothelium in neonatal rats. Invest Ophthalmol Vis Sci 1998, 39:2572–2583
50. Shimura-Miura H, Hattori N, Kang D, Miyako K, Nakabeppu Y, Mizuno Y: Increased 8-oxo-dGTPase in the mitochondria of substantia nigral neurons in Parkinson's disease. Ann Neurol 1999, 46:920–924
51. Mecocci P, MacGarvey U, Beal MF: Oxidative damage to mitochondrial DNA is increased in Alzheimer's disease. Ann Neurol 1994, 36:747–751
52. Yakes FM, Van Houten B: Mitochondrial DNA damage is more extensive and persists longer than nuclear DNA damage in human cells following oxidative stress. Proc Natl Acad Sci USA 1997, 94:514–519
53. Reddy VN, Kasahara E, Hiraoka M, Lin LR, Ho YS: Effects of variation in superoxide dismutases (SOD) on oxidative stress and apoptosis in lens epithelium. Exp Eye Res 2004, 79:859–868
54. Banmeyer I, Marchand C, Clippe A, Knoops B: Human mitochondrial peroxiredoxin 5 protects from mitochondrial DNA damages induced by hydrogen peroxide. FEBS Lett 2005, 579:2327–2333
55. Tuberville AW, Wood TO, McLaughlin BJ: Cytochrome oxidase activity of Fuchs' endothelial dystrophy. Curr Eye Res 1986, 5:939–947